

Supporting Information of

Stabilization of two-dimensional penta-silicene for flexible lithium-ion battery anodes via surface chemistry reconfiguration

Donghai Wu^a, Shuaiwei Wang^a, Shouren Zhang^a, Yibiao Liu^a, Yingchun Ding^c,
Baocheng Yang^a, Houyang Chen^{b*}

^a Henan Provincial Key Laboratory of Nanocomposites and Applications, Institute of Nanostructured Functional Materials, Huanghe Science and Technology College, Zhengzhou 450006, China

^b Department of Chemical and Biological Engineering, State University of New York at Buffalo, Buffalo, New York 14260-4200, USA

^c College of Optoelectronics Technology, Chengdu University of Information Technology, Chengdu, 610225, China

* To whom correspondence should be addressed. Email: hchen23@buffalo.edu

Section S1. Theoretical methods

All first-principles calculations were implemented in the Vienna *ab-initio* Simulation Package (VASP) with the projector augmented wave (PAW) method.¹ The exchange-correlation potential was described by the generalized gradient approximation (GGA) within the Perdew-Burke-Ernzerhof (PBE)² functional. Additionally, the hybrid Heyd-Scuseria-Ernzerhof (HSE06) functional³ was also introduced to calculate more accurate band structures. The plane-wave basis with a cutoff energy of 600 eV is used. A well-tested k-point mesh of $9 \times 9 \times 1$ in the Monkhorst-Pack sampling scheme⁴ was adopted. The geometric structures were fully relaxed until the total energy was less than 10^{-5} eV and the force reached the convergence threshold of 0.01 eV/Å. The van der Waals correction was included using the DFT-D3 method.⁵ The phonon spectra were calculated employing the Phonopy program⁶ through the finite difference method. Considering the periodic boundary conditions, a vacuum space of 20 Å was included to avoid interactions between adjacent images. A $2 \times 2 \times 1$ supercell was modeled for the investigation of Li atom adsorption and diffusion processes, to avoid the clustering between the adjacent Li atoms. The climbing-image nudged elastic band (CI-NEB) method⁷ was applied to find an energy optimized pathway between two nearest energy minima for the investigation of Li diffusion behaviors on the surface of the fully fluorinated penta-silicene.

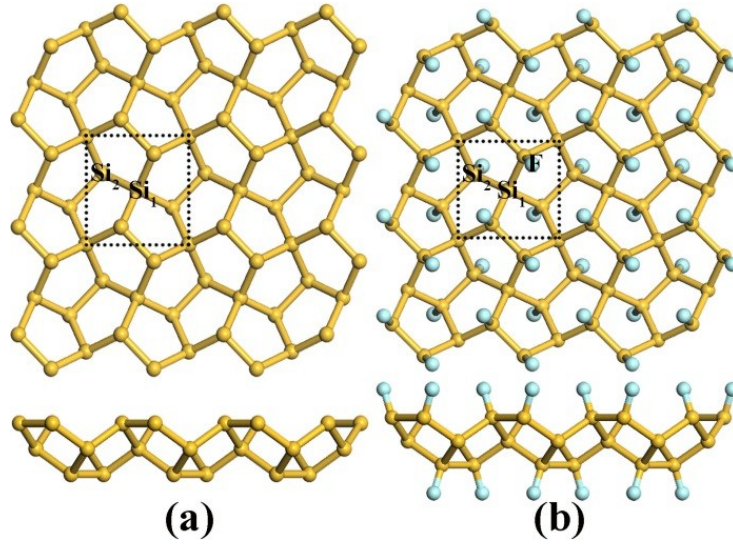


Figure S1. Top (upper) and side views (below) of the optimized pristine penta-silicene (a) and fully fluorinated penta-silicene (b).

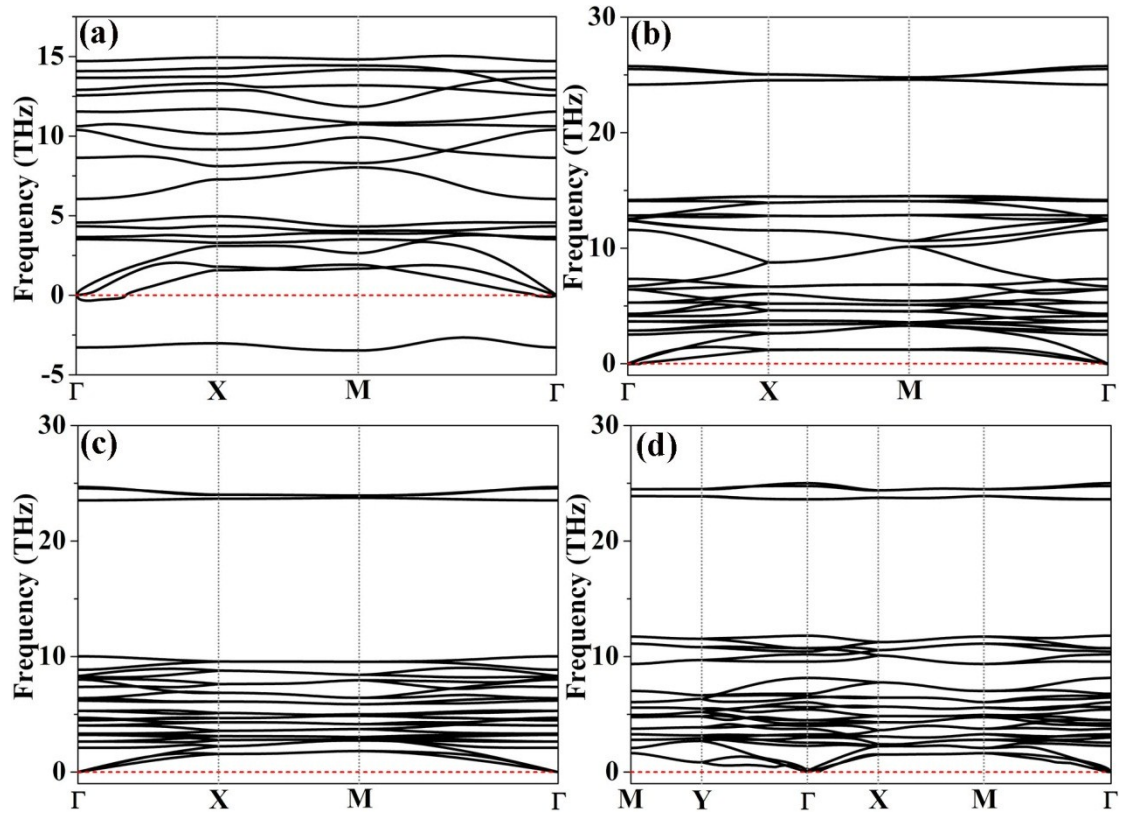


Figure S2. The phonon spectra of the pristine penta-silicene (a), the fully fluorinated penta-silicene (b), the fully fluorinated penta-silicene sheet under biaxial strain of 0.23 (c), and the fully fluorinated penta-silicene sheet under uniaxial strain of 0.30 (d).

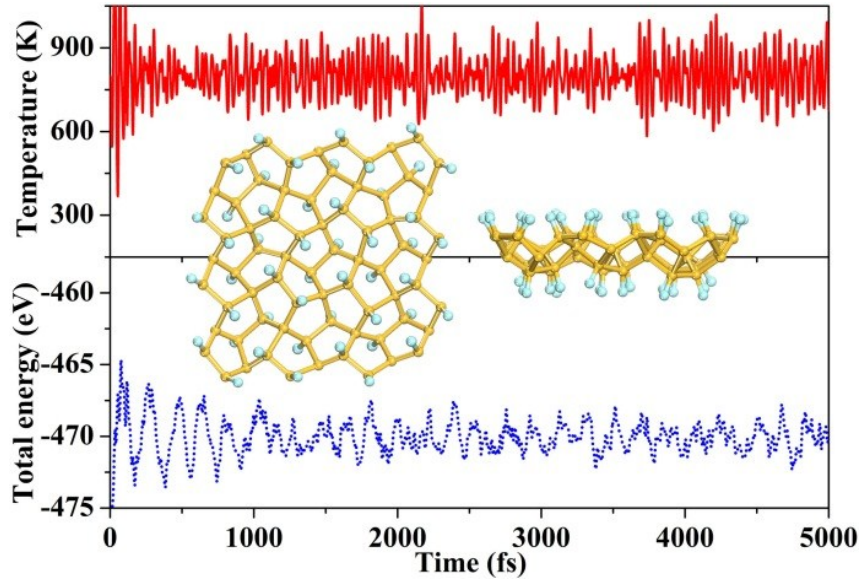


Figure S3. Fluctuations of temperature and total energy for a fully fluorinated penta-silicene sheet at 800 K. Insets are top and side views of the final structure after the simulation.

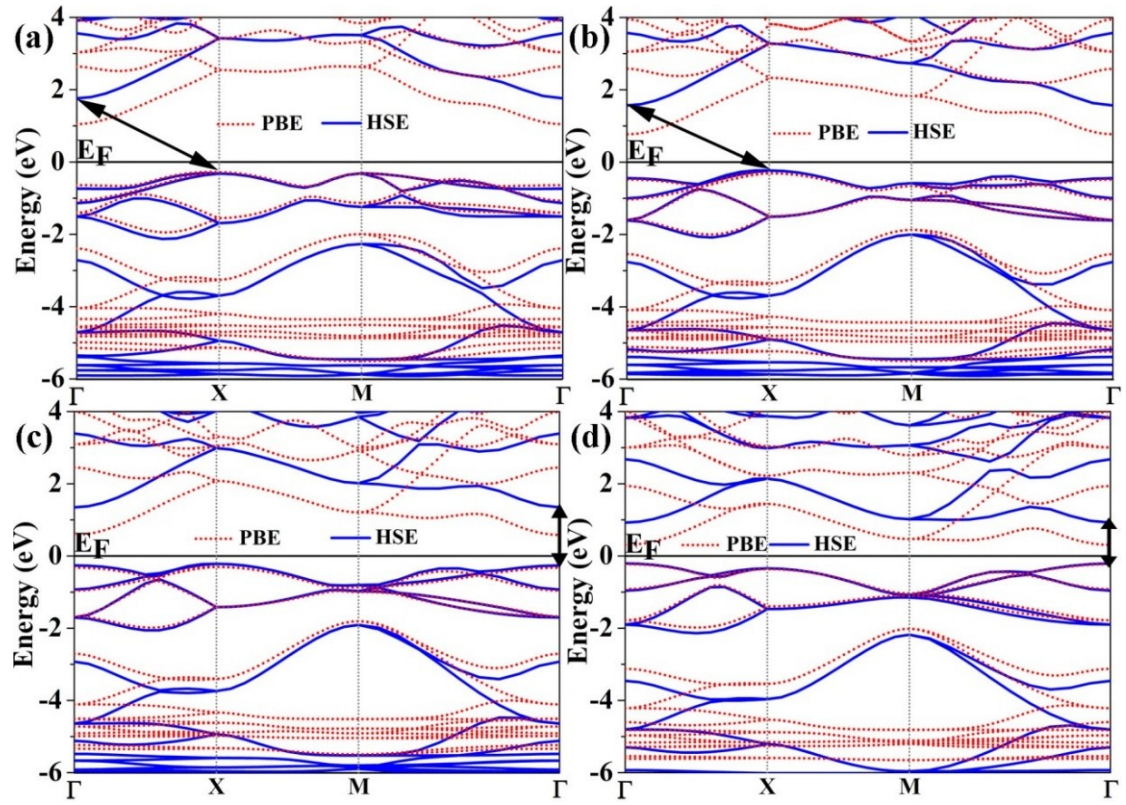


Figure S4. Band structures from PBE and HSE functionals of fully fluorinated penta-silicene sheet under biaxial strains of 0.05 (a), 0.10 (b), 0.15 (c), and 0.23 (d).

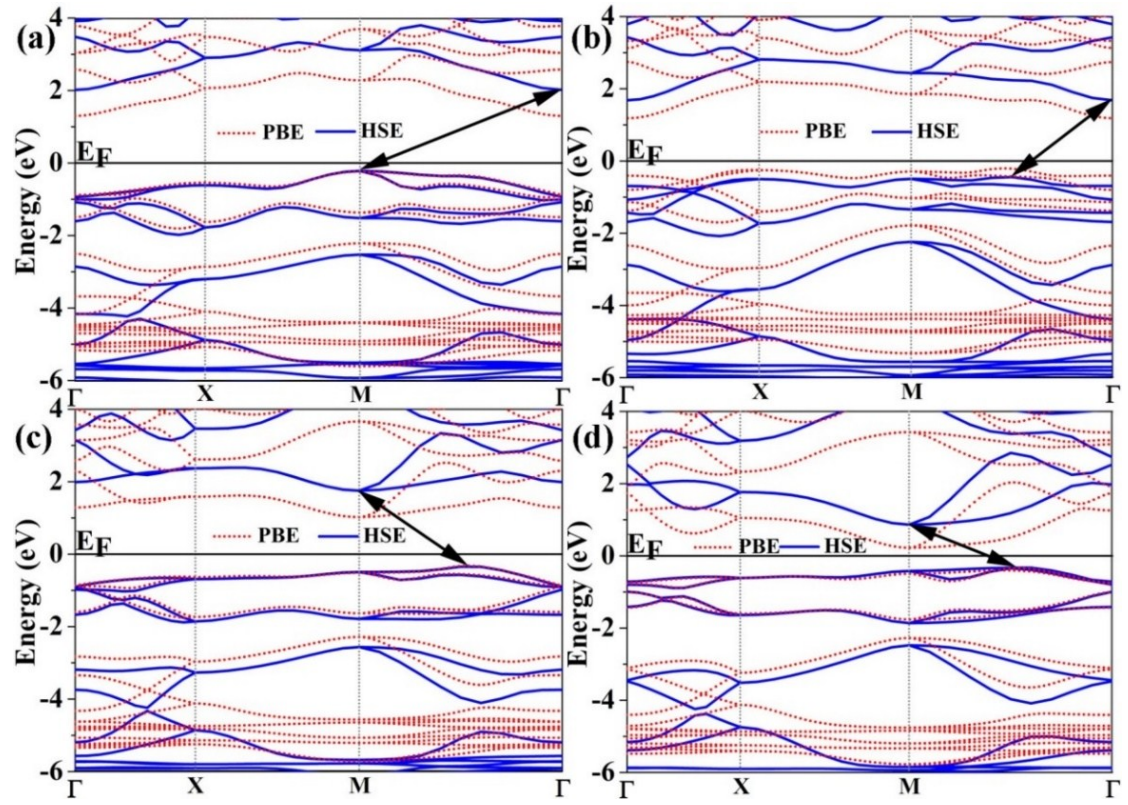


Figure S5. Band structures from PBE and HSE functionals of fully fluorinated penta-silicene sheet under uniaxial strains of 0.10 (a), 0.15 (b), 0.20 (c), and 0.30 (d).

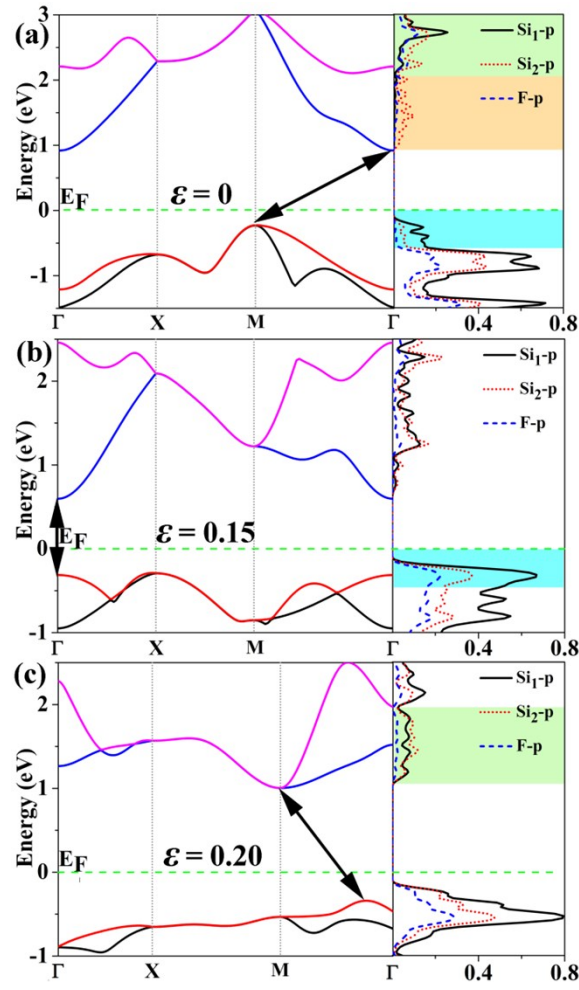


Figure S6. The band structures and corresponding PDOS from PBE functional of a fully fluorinated penta-silicene sheet under strain-free (a), biaxial strain of 0.15 (b) and uniaxial strain of 0.20 (c).

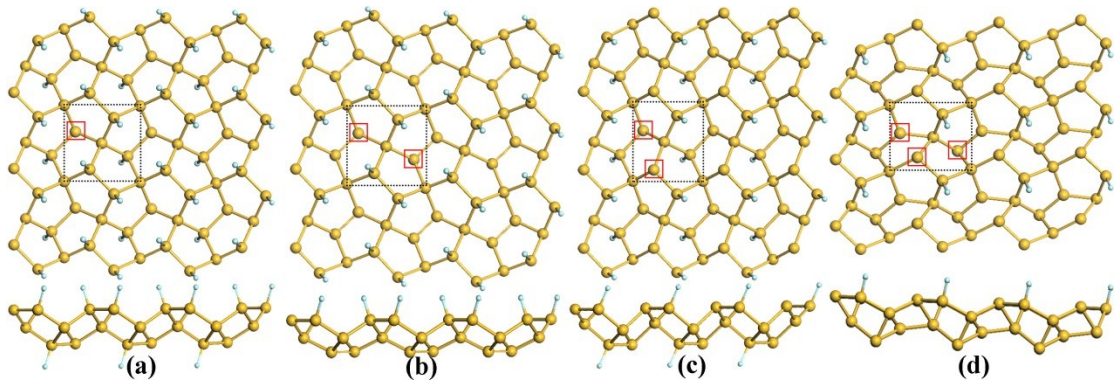


Figure S7. Top (upper) and side views (below) of the optimized configurations of partially fluorinated penta-silicene sheets Si_6F_3 (a), Si_6F_2 -I (b), Si_6F_2 -II (c), and Si_6F (d). Red squares represent the tricoordinated Si atom without decorating F atoms.

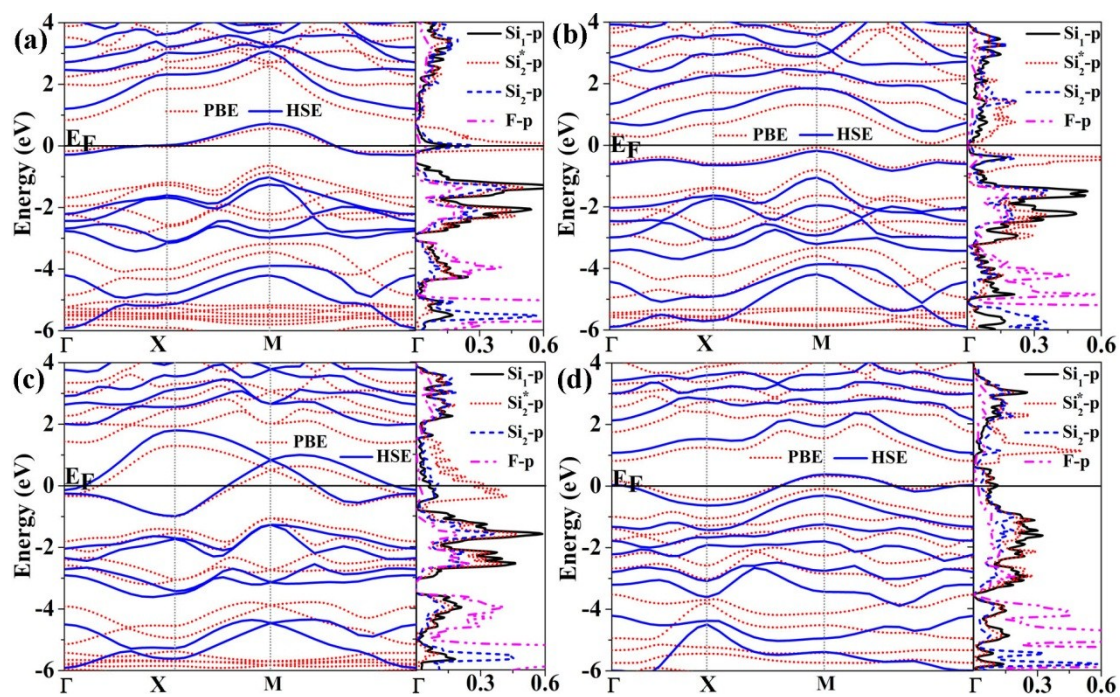


Figure S8. Band structures and corresponding PDOS from PBE and HSE functionals of partially fluorinated penta-silicene sheets of Si_6F_3 (a), $\text{Si}_6\text{F}_2\text{-I}$ (b), $\text{Si}_6\text{F}_2\text{-II}$ (c), and Si_6F (d). In PDOS, $\text{Si}^* 2$ denotes the tricoordinated Si atom without decorating F atoms, labeled with red squares in Figure S7.

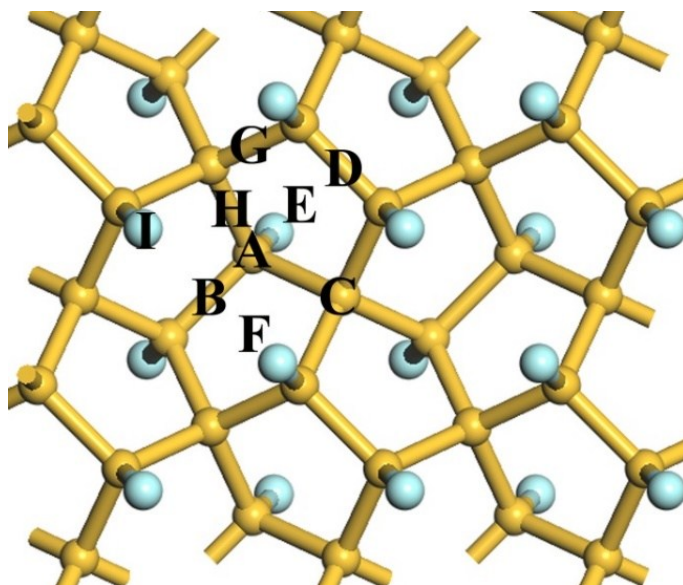


Figure S9. Schematic diagram of all possible adsorption sites for a Li atom on a fully fluorinated penta-silicene sheet.

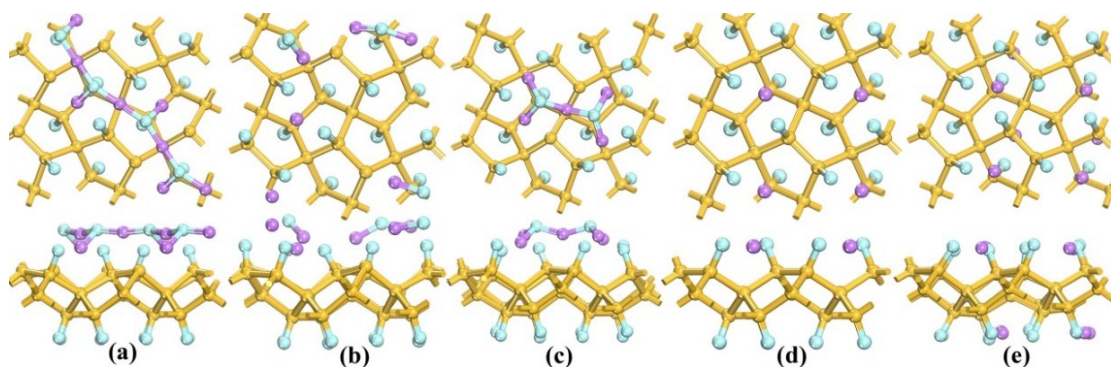


Figure S10. Top (upper) and side views (below) of the possible configurations for multiple Li atoms adsorption on the fully fluorinated penta-silicene on one (a-d) and two sides (e) after structural optimization. (a) Eight Li atoms, (b) six Li atoms, (c) five Li atoms, and (d) four Li atoms. (e) Four Li atoms in each side (Total eight on both sides). Our results showed that four Li atoms could be adsorbed steadily on one side of the sheet(d), whereas 5-8 atoms could not be adsorbed steadily (a-c). Eight atoms could be adsorbed steadily on both sides of the sheets (e).

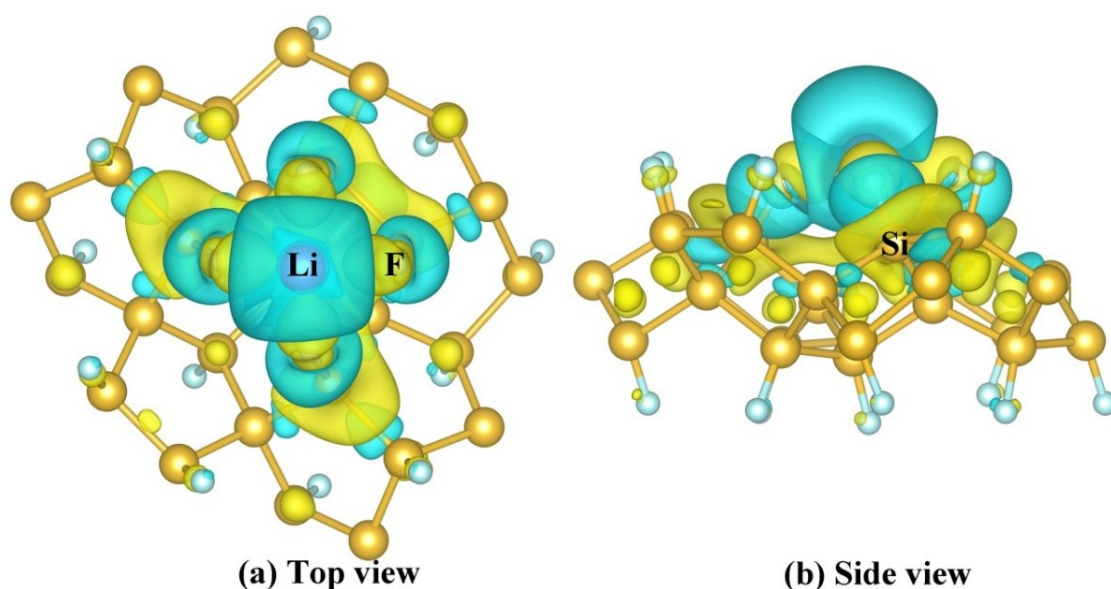


Figure S11. Top (a) and side (b) views of charge density difference for the single Li adsorption on a fully fluorinated penta-silicene sheet. Cyan and yellow regions represent the electron losses and gains, respectively.

1. G. Kresse and J. Furthmüller, *Phys. Rev. B*, 1996, **54**, 11169-11186.
2. J. P. Perdew, K. Burke and M. Ernzerhof, *Phys. Rev. Lett.*, 1996, **77**, 3865-3868.
3. J. Heyd, G. E. Scuseria and M. Ernzerhof, *J. Chem. Phys.*, 2003, **118**, 8207-8215.
4. H. J. Monkhorst and J. D. Pack, *Phys. Rev. B*, 1976, **13**, 5188-5192.
5. S. Grimme, J. Antony, S. Ehrlich and H. Krieg, *J. Chem. Phys.*, 2010, **132**, 154104.
6. A. Togo and I. Tanaka, *Scripta Mater.*, 2015, **108**, 1-5.
7. D. Sheppard, R. Terrell and G. Henkelman, *J. Chem. Phys.*, 2008, **128**, 134106.